Available online at www.sciencedirect.com
ScienceDirect
Journal of the European Ceramic Society 31 (2011) 1405–1412
www.elsevier.com/locate/jeurceramsoc

Magnetic field oriented tetragonal zirconia with anisotropic toughness

Li Zhang [a,*], Jef Vleugels [a], Larysa Darchuk [b], Omer Van der Biest [a]

[a] Department of Metallurgy and Materials Engineering, Katholieke Universiteit Leuven, Kasteelpark Arenberg 44, Heverlee, Leuven BE-3001, Belgium
[b] Department of Chemistry, University of Antwerpen, Universiteitsplein 1, Wilrijk BE-2610, Belgium

Received 31 August 2010; received in revised form 16 January 2011; accepted 3 February 2011
Available online 5 March 2011

Abstract

(0 0 1)-oriented 3 mol% yttria stabilized tetragonal zirconia (3Y-TZP) has been developed by reactive synthesis of undoped pure monoclinic zirconia and co-precipitated 8 mol% yttria-stabilized zirconia (8Y-ZrO_2). The dispersed pure monoclinic ZrO_2 powder, having magnetic anisotropy, was first aligned in a strong magnetic field and co-sintered in a randomly distributed cubic 8Y-ZrO_2 fine matrix powder. The reactive sintering resulted in a 3Y-TZP ceramic with a (0 0 1) orientation. The (0 0 1)-oriented 3Y-TZP showed a substantial toughness anisotropy, i.e. the toughness along the [0 0 1] direction is 54% higher than that of its perpendicular direction. Moreover, the toughness along the [0 0 1] direction is 49% higher than that of a non-textured isotropic reactively synthesized 3Y-TZP and 110% higher than that of an isotropic co-precipitated powder based 3Y-TZP. The substantially enhanced toughness was interpreted in terms of the tetragonal to monoclinic martensitic phase transformability.

Keywords: Suspensions; Magnetic alignment; Sintering; Toughness and toughening; ZrO_2

1. Introduction

Zirconia ceramics are one of the most important engineering ceramics and are widely used in various applications such as thermal barrier coatings for high temperature protection, solid electrolytes for oxygen sensors, high-temperature fuel cells, and recently dental material.[1,2] Zirconia ceramics have become increasingly popular due to their unusual combination of strength, fracture toughness, ionic conductivity, and low thermal conductivity.[3] The most attractive feature of zirconia is its high fracture toughness (2–10 MPa $m^{1/2}$).[4] This is dominantly attributed to the stress induced transformation of the tetragonal to monoclinic phase in the stress field of the propagating cracks, i.e. a phenomenon well known as 'transformation toughening'.[1,3–6] Transformation toughening is considered to be the dominant toughening mechanism of partially stabilized ZrO_2 and extensive efforts have been devoted to understand the transformability of tetragonal zirconia. However, most studies have focused on polycrystalline ZrO_2 ceramics without any orientation, and there are hardly reports on the textured ZrO_2 ceramics.

Textured ceramics have attracted much interest due to their improved properties. Various techniques, like hot forging, deformation and templated grain growth are commonly used to produce textured ceramics.[7–9] With the development of superconducting magnets, the alignment of feeble non-cubic magnetic particles, such as Al_2O_3, ZnO, TiO_2, SiC and Si_3N_4, becomes possible in strong magnetic fields.[10,11] Taking α-alumina as an example, hexagonal single crystal alumina particles in a low viscosity suspension can be aligned in a strong magnetic field (~10 T) when the magnetic crystal anisotropy energy ΔE is larger than the energy of thermal motion:[10,12]

$$\Delta E > k_B T \tag{1}$$

with k_B the Boltzmann constant and T the absolute temperature. The crystal anisotropy energy ΔE in a magnetic field is expressed by:

$$\Delta E = -\frac{\Delta\chi V B^2}{2\mu_0} \tag{2}$$

where $\Delta\chi = \chi_{a,b} - \chi_c$ is the anisotropy of the magnetic susceptibility, with $\chi_{a,b}$ the magnetic susceptibility along the crystallographic a- or b-axes and χ_c the magnetic susceptibility along the crystallographic c-axis of alumina, μ_0 is the perme-

* Corresponding author. Tel.: +32 16 32 17 77; fax: +32 16 32 19 92.
E-mail addresses: li.zhang@mtm.kuleuven.be, zhllli2001@hotmail.com (L. Zhang).

0955-2219/$ – see front matter © 2011 Elsevier Ltd. All rights reserved.
doi:10.1016/j.jeurceramsoc.2011.02.002

ability of vacuum, B is the applied magnetic field and V is the particle volume.

In this study, the possibility of texturing zirconia using a strong magnetic field was assessed and subsequently the mechanical properties of the obtained textured zirconia were evaluated. The objective of this study was to achieve textured 3 mol% yttria-stabilized tetragonal zirconia (3Y-TZP), which can be used in many applications.[4,13] Since it was reported that 3 mol% co-precipitated ZrO_2 powder was negligibly oriented in a magnetic field of 12 T,[13,14] we aimed at the alignment of pure undoped monoclinic zirconia (m-ZrO_2) in a starting powder suspension of pure m-ZrO_2 and co-precipitated 8 mol% yttria-stabilized zirconia (8Y-ZrO_2) in a strong magnetic field to obtain a textured 3Y-TZP after sintering to full density.

2. Experiment

Unstabilized m-ZrO_2 (SF-extra grade, Z-Tech LLC, USA) and co-precipitated 8Y-ZrO_2 (TZ-8Y grade, Tosoh Co., Japan) were used as the starting powder. For comparison, a commercial co-precipitated 3Y-TZP powder (TZ-3Y grade, Tosoh Co., Japan, Fig. 1(a) and (c)) was also used. A mixture of SF-extra/TZ-8Y (mixed 3Y-TZP grade) with a molar ratio of 5:3 was mixed and deagglomerated by bead milling (Dispermat SL, VMA Getzmann GmbH, Germany) in ethanol at 6000 rpm for 4 h using zirconia beads with an average size of 1 mm (TZ-3Y, Tosoh Co, Japan). The morphology and particle size distribution of the mixed powder after bead milling is shown in Fig. 1(b) and (d). The particle size of SF-extra and 8Y-ZrO_2 powders were also measured separately and the average particle sizes were calculated according to the statistics. It was determined that the monoclinic SF-extra powder has an average particle size of 205 nm, while the TZ-8Y powder has an average particle size of 75 nm after deagglomeration by bead milling.

To prepare a stable suspension, the milled powder (powder load 250 g/L) was dispersed with 1 wt% (relative to the powder load) phosphate ester (JP-506H grade, Johoku Chem. Co. Ltd, Japan) as charging agent and binder. Pre-test experiments showed that the addition of 1.1 wt% (relative to the powder load) poly(vinyl butyral-*co*-vinyl alcohol-*co*-vinyl acetate) (PVB, Sigma-Aldrich Corp., USA) as binder and 0.03 wt% (relative to the powder load) polyethyleneimine (PEI, Sigma-Aldrich Corp., USA) as surface charging agent and stabilizer was effective to form a thick and crack-free deposit.[15] The mixed zirconia powder was deposited from the freshly prepared suspension by electrophoretic deposition (EPD). A horizontal strong magnetic field of 9.4 T (Bruker, Germany) was applied to the suspension during EPD at room temperature with parallel magnetic and electric field directions. In other words, the deposition electrode was placed vertically and was perpendicular to the magnetic field. For comparison, the mixed 3Y-TZP grade as well as the commercial co-precipitated TZ-3Y grade was prepared by EPD outside the magnet. Moreover, in order to check the alignment of the m-ZrO_2 powder, an SF-extra powder suspension was investigated with and without magnetic field.

The green compacts were dried outside of the magnet and sintered in air at 1500 °C for 3 h (Nabertherm, Germany). The sintered zirconia ceramics were analyzed by scanning electron microscopy (SEM, XL30-FEG, FEI, The Netherlands) and X-ray diffraction (XRD, Seifert 3003T/T, Germany) to evaluate the microstructure and texture formation. Grain size distributions were obtained from the linear intercepts of 130 grains measured on the well dispersed powder or on the thermally etched surfaces. The grain size data are presented as measured since no mathematical corrections were performed.

The Lotgering factor, based on XRD spectral analysis, was used to quantify the degree of orientation. The Lotgering factor, f, is defined as:[16]

$$f = \frac{P - P_0}{1 - P_0} \tag{3}$$

with $P = I_{100}/\Sigma I_{hkl}$ and $P = I_{001}/\Sigma I_{hkl}$ for monoclinic and tetragonal ZrO_2, respectively. P_0 is calculated from a randomly oriented sample according to the same formula. I_{hkl} is the peak intensity of all the $h\,k\,l$ reflections in the 20–80° 2θ range. The f factor of an isotropic material is 0, while f equals 1 for a single crystal. The Lotgering factor, f, is considered to be an estimate of the degree of orientation in the textured material.

The Vickers hardness (HV_5) of the sintered ceramics was measured (Model FV-700, Future-Tech Corp., Japan) on polished surfaces with an indentation load of 5 kg. Vickers hardness indent to measure fracture toughness (K_{Ic}) has been widely used and analyzed due to the relative ease of the technique.[17] A useful analysis method in the determination of K_{Ic} from Vickers indent in tetragonal zirconia (t-ZrO_2) polycrystalline ceramics was proposed by Anstis et al.[18] The K_{Ic} was calculated from the diagonal length of the radial cracks originating in the corners of the Vickers indentations, according to the formula:[18]

$$K_{Ic} = 0.0154\sqrt{\frac{E}{H_V}}\left(\frac{P}{c^{1.5}}\right)\ (\mathrm{MPa\ m^{1/2}}) \tag{4}$$

with E, the Young's modulus (GPa), H_V, the Vickers hardness (GPa), P the indentation load (N) and c, half of the total crack length (m). For the ceramic deposited in the magnetic field, the indent was oriented so that one of its diagonals was parallel to the magnetic field direction. For anisotropic materials, the diagonal length of the radial cracks in a specific direction was measured to derive the K_{Ic} for cracks propagating in that direction. The E value used in the calculation according to Eq. (4) is 210 GPa. The reported hardness and toughness values are the average and standard deviation for five indentations.

The ZrO_2 phase transformation at the crack tip of the Vickers indentations was analyzed with an InVia micro Raman spectrometer (Renishaw, Wotton-under-Edge, UK), equipped with an argon laser (514.5 nm, Spectra Physica, The Netherlands) with a maximum laser power of 50 mW. The spectra were obtained with a 50× magnification objective.

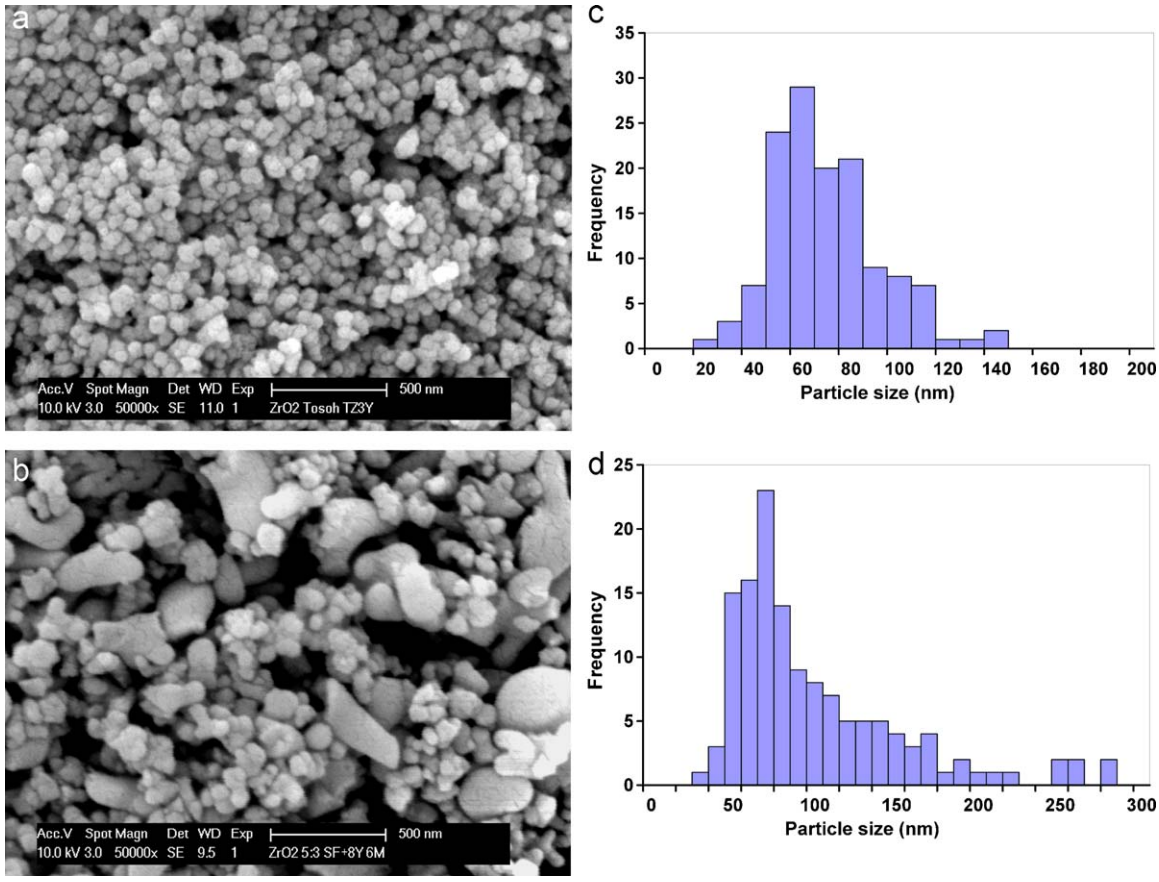

Fig. 1. SEM micrographs and corresponding particle size distributions of the co-precipitated 3Y-TZP (a, c) and the mixed SF-extra/TZ-8Y (b, d) starting powder.

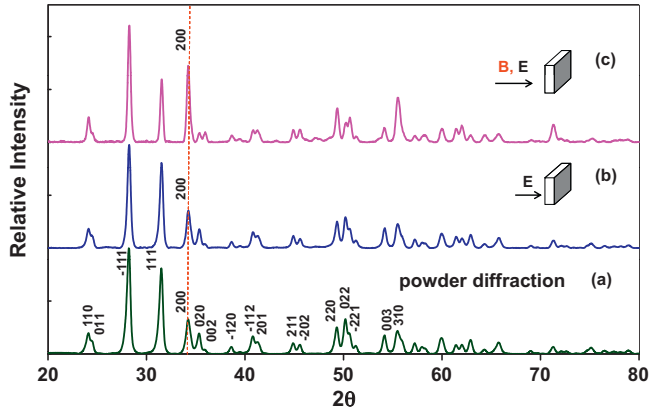

Fig. 2. XRD spectra of the SF-extra m-ZrO_2 starting powder (a) and sintered body, deposited in the absence (b) and in the presence (c) of the magnetic field. E and B indicate the direction of the electric and magnetic field with respect to the diffraction surface.

3. Results and discussion

3.1. Texture development

The XRD spectra of the sintered SF-extra m-ZrO_2 deposits in the absence and presence of a magnetic field are compared in Fig. 2, together with the starting powder spectrum for comparison. The influence of the magnetic field can be assessed by comparing the ceramics deposited with and without magnetic field. The spectrum of the starting powder shown in Fig. 2(a) is the same as that of the sintered ceramic deposited in the absence of a magnetic field (Fig. 2(b)), both of which perfectly match the m-ZrO_2 reference spectrum (JCPDS card number 37-1484). This indicates that the grains are not aligned in the ZrO_2 ceramic deposited without magnetic field.

In contrast, the alignment of m-ZrO_2 by magnetic field was confirmed by XRD, as shown in Fig. 2(c), where the 2 0 0 diffraction peak intensity is very pronounced when measured from the surface perpendicular to the magnetic field. This implies that the magnetic field influences the m-ZrO_2 ($a = 5.203$ Å, $b = 5.217$ Å, $c = 5.388$ Å, and $\beta = 98.91°$)[3] particle alignment during EPD, i.e. the (1 0 0) plane of the m-ZrO_2 particles is aligned perpendicular to the magnetic field direction and this alignment can be retained to some extent after sintering. However, the preferred crystal orientation in the sintered m-ZrO_2 is limited, and the Lotgering factor is only 0.05. This may be related to the phase transformation occurring during the sintering process. The monoclinic (m) to tetragonal (t) (m → t) transformation in pure ZrO_2 occurs at ~1150 °C during heating and is reversible (t → m) at ~950 °C during cooling.[19] The t → m transformation is accompanied by a large shear strain (~0.16) and a significant volume expansion (~4%).[19] Due to the large internal stresses created during cooling, it is widely observed that the unstabilized pure zirconia sintered above 1150 °C inevitably

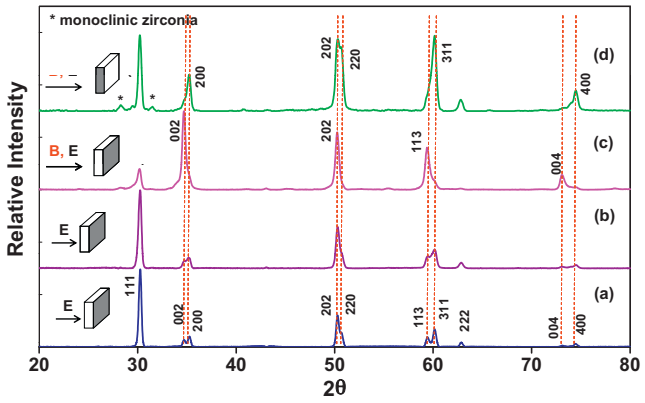

Fig. 3. XRD spectra of the sintered co-precipitated 3Y-TZP (a) and SF-extra/TZ-8Y mixed (b) powder processed in the absence of a magnetic field, together with the diffraction patterns of the mixed SF-extra/TZ-8Y powder of the surface perpendicular (c) and parallel (d) to the magnetic field.

disintegrates by cracking upon cooling.[3] The SF-extra monoclinic zirconia, with EPD outside of the magnetic field, indeed became a weak powder compact after sintering at 1500 °C and could be easily broken and crushed. The volume change accompanying the t → m transformation results in spontaneous transformation, micro-cracking and material disintegration. This also happened to the (1 0 0)-oriented pure ZrO_2, although its expansion mismatch is expected to be smaller than the random equivalent. More importantly, during this t → m martensitic transformation, the orientation of the aligned ZrO_2 grains may be destroyed. Hayakawa et al. studied the t → m transformation in arc-melted 2 mol% Y_2O_3 doped ZrO_2 by using X-ray diffraction, optical metallography and transmission electron microscopy.[20–22] They found that 12 possible variants of the monoclinic phase can originate from one single tetragonal grain. Due to the multiple variants, the orientation relationship between the tetragonal parent and monoclinic product phases becomes complex and the orientation of the polycrystalline ZrO_2 cannot be well preserved after the t → m transformation, which resulted in limited orientation in the sintered sample.

To prevent the spontaneous transformation during cooling, yttria was introduced to stabilize the t-ZrO_2 phase. The XRD spectra of the sintered 3Y-TZP ceramics processed in the absence and presence of a magnetic field are compared in Fig. 3. The XRD spectra of the sintered co-precipitated and mixed powder based 3Y-TZP ceramics, prepared in the absence of a magnetic field and measured on the surface perpendicular to the electric field, are shown in Fig. 3(a) and (b) respectively. Both spectra match the reference t-ZrO_2 spectrum (JCPDS card number 17-0923) perfectly, indicating that isotropic 3Y-TZP ceramics were obtained after reactive sintering. In contrast, an anisotropic 3Y-TZP was obtained when conducting the EPD in a strong magnetic field. As shown in Fig. 3(c), the 0 0 2 and 0 0 4 diffraction peaks of the mixed powder based ceramic were much enhanced when measured on the surface perpendicular to the magnetic field direction. On the contrary, those peaks almost disappeared from the spectrum of the surface parallel to the magnetic field (Fig. 3(d)), whereas the 2 0 0, 2 2 0 and 4 0 0 diffraction peaks became significant. Accordingly, the Lotgering factor of the reactively sintered 3Y-TZP is 0.36. It can be concluded that a (0 0 1)-oriented 3Y-TZP was formed after reactive sintering of the mixed powder compact deposited in a magnetic field.

The t-ZrO_2 grain alignment should be directly related to the magnetically aligned m-ZrO_2 grains in the starting powder. The texture in the 3Y-TZP is substantially higher than that of the pure m-ZrO_2 discussed above. Since the 3Y-TZP does not undergo the t → m transformation during cooling, this also confirms that the t → m transformation of the pure m-ZrO_2 is detrimental to the crystallographic texture. It is also noted that in Fig. 3(d), besides the diffraction peaks of t-ZrO_2, there are two small m-ZrO_2 peaks, which were the result of the well known t → m martensitic transformation on the surface due to the stresses generated during grinding and polishing for sample preparation.[3,6,19] This also indicates that the powder mixture based 3Y-TZP is a highly transformable ZrO_2 ceramic since the transformation cannot be completely avoided during an appropriate polishing, as is the case for the co-precipitated 3Y-TZP powder based material (see Fig. 3(a)). Surprisingly, the amount of m-ZrO_2 in the powder mixture based grade processed in a magnetic field is surface dependent (compare Fig. 3(c) and (d)) and no m-ZrO_2 was observed on the surface of the mixed powder based ceramic processed in the absence of a magnetic field (Fig. 3(b)).

From the above observations, it can be concluded that the $(0\,0\,1)_t$ plane was aligned perpendicular to the magnetic field and the orientation relationship between the monoclinic precursor phase and the obtained tetragonal phase is $(1\,0\,0)_m//(0\,0\,1)_t$, where $(1\,0\,0)_m$ is the (1 0 0) plane of m-ZrO_2 phase and $(0\,0\,1)_t$ is the (0 0 1) plane of the t-ZrO_2 phase. The 8 mol% yttria stabilized cubic TZ-8Y precursor powder cannot be aligned in a magnetic field due to its magnetic isotropy.[11] This would also imply that there is hardly any significant grain rearrangement during sintering. This is similar to the result reported by Suárez et al.,[14] where the aligned monomodal sized m-ZrO_2 grains (TZ-0 grade, Tosoh Co., Japan, primary particle size 75.8 nm) are transformed into 3Y-TZP by reacting with yttrium oxide, although the alignment was not significant. The better alignment of the powder mixed 3Y-TZP in this work may be attributed to the particle size difference between the SF-extra and TZ-8Y powders (Fig. 1(b) and (d)). As reported, the interaction of particles during consolidation or deposition may destroy the crystallographic alignment of particles and a bimodal particle size distribution of the mixed powder can minimize this effect.[23] The larger SF-extra grade ZrO_2 particles are also more prone to alignment, as indicated by Eq. (1), and react with the randomly distributed TZ-8Y fine powder during sintering to form a stable 3Y-TZP ceramic. This is analogous to the "reactive templated grain growth" (RTGG), which is recently developed to texture materials.[24] In RTGG, the anisotropically shaped precursor particles, acting as reactive-templates, are aligned in a powder matrix during consolidation. During sintering, the template particles react with the matrix powder and form a new phase. Simultaneously, the new phase will take the orientation from the precursor, thus form a textured material. RTGG have been successfully applied in several compounds, whose templates with the same composition are difficult to make, such as $Bi_{0.5}Na_{0.5}TiO_3$ (BNT)-based ceramics, $CaBi_4Ti_4O_{15}$ and $NaCo_2O_4$.[24–26] In the present study, the

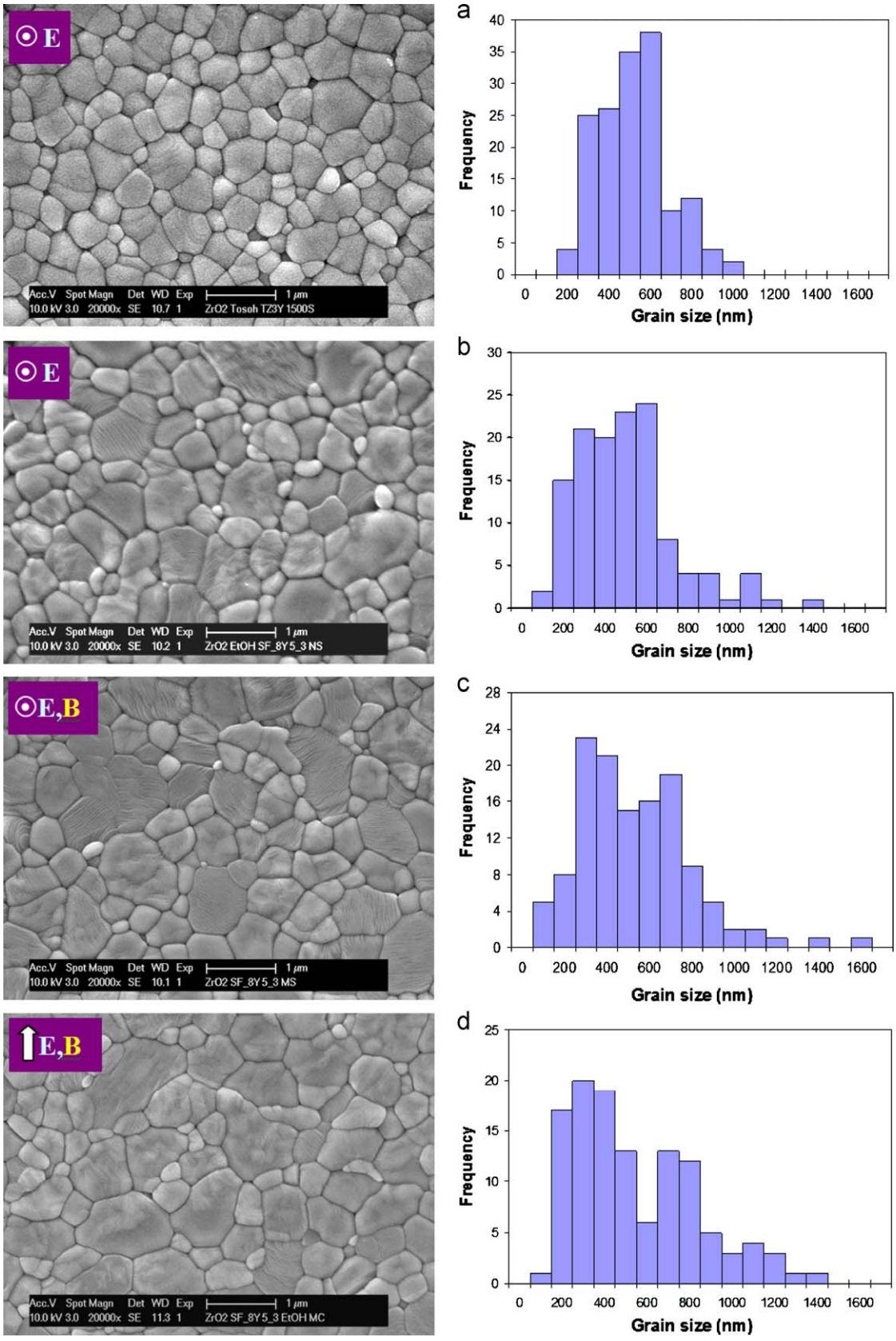

Fig. 4. Microstructure of thermally etched surfaces and corresponding grain size distribution of the co-precipitated (a) and the mixed (b, c, d) powder based 3Y-TZP. The direction of the electric, E, and/or magnetic, B, field are indicated on the images.

Table 1
Mechanical properties of the co-precipitated and mixed powder based 3Y-TZP, prepared in the absence or in the presence of magnetic field.

3Y-TZP	Magnetic field	Direction	Hardness HV_5 (kg/mm^2)	Toughness K_{Ic} (MPa m$^{1/2}$)
Co-precipitated	No	Random	1292 ± 13	4.0 ± 0.1
Mixed powder based	No	Random	1258 ± 18	5.9 ± 0.1
	Yes	Along [0 0 1]	1228 ± 12	8.8 ± 0.5
	Yes	Along⊥ [0 0 1]	1208 ± 12	5.7 ± 0.3

SF-extra grade monoclinic particles, acting as precursor, have irregular shape and are aligned by the magnetic field due to their anisotropic magnetic susceptibility. During sintering, they react with the matrix TZ-8Y powder and form a new 3Y-TZP phase, which inherits their orientation.

3.2. Microstructure evolution

The microstructure and corresponding grain size distributions of the co-precipitated powder and SF-extra/TZ-8Y mixed powder based 3Y-TZP, sintered at exactly the same conditions, are compared in Fig. 4. As shown in Fig. 4(a), the co-precipitated 3Y-TZP has a monomodal grain size distribution within the 200–1000 nm range with an average grain size of 380 nm. In contrast, the mixed powder based 3Y-TZP ceramics whether processed in the absence (Fig. 4(b)) or in the presence (Fig. 4(c) and (d)) of a magnetic field show a much wider grain size distribution with a small fraction of grains >1000 nm and <200 nm. The average grain size of the reactively synthesized 3Y-TZP is 450 nm, which is larger than that of the co-precipitated powder based equivalent.

The grain size of a sintered deposit consisting of only m-ZrO_2 is ~4 μm, which is much larger than that of the mixed powder based 3Y-TZP (0.45 μm). As reported by Gupta et al.,[4] TZ-8Y powder pellet sintered at 1450 °C for 2 h had a grain size in the range of 2–5 μm. Apparently, the mixed powder inhibits the grain growth, which is related to the diffusion of yttrium in zirconia. The grain size of yttria stabilized ZrO_2 is a direct function of the yttria content and distribution.[27,28] The ZrO_2 grain size is large for unstabilized monoclinic ZrO_2, decreases with increasing yttria to a minimum grain size in the 2–3 mol% yttria range, and increases again at higher yttria contents.[28] The yttria redistribution during sintering limits the grain size and forms a 3Y-TZP. The wider grain size distribution of the mixed powder based 3Y-TZP is a result of the wider particle size distribution of the mixed starting powder, shown in Fig. 1(b) and (d), and the yttria redistribution limiting grain growth during sintering. The larger grains can be directly correlated to the larger fraction of m-ZrO_2 grains in the starting powder, implying that these grains are larger due to their lower yttria content. Moreover, larger grains with lower yttria content have a higher transformability and will boost up the fracture toughness of the material (mixed versus co-precipitated grade), providing they do not spontaneously transform.

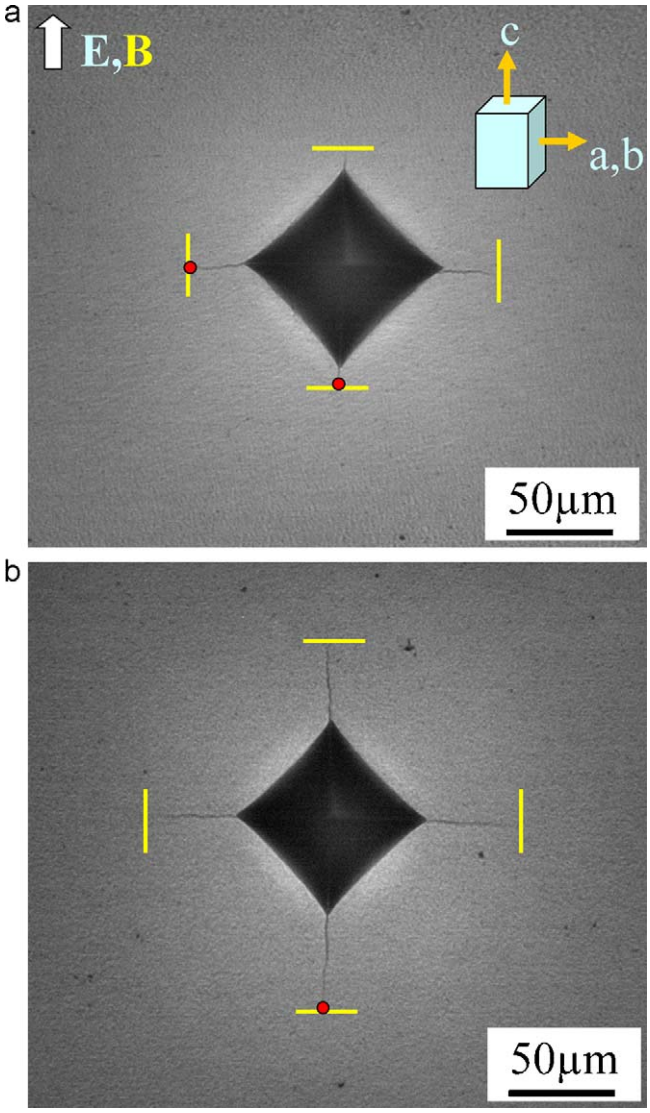

Fig. 5. Vickers indentations and radial crack patterns on the mixed (a) and co-precipitated (b) powder based 3Y-TZP. The direction of the electric, E, and magnetic, B, field are indicated on the images. The ends of the crack are marked with a straight line to make it visible. The spots marked at the end of crack are the positions where micro Raman (Fig. 6) measurements are performed.

The microstructure of the textured, mixed powder based 3Y-TZP (Fig. 4(c) and (d)) was quite similar to that of the random one (Fig. 4(b)) deposited outside of the magnet. The microstructures of the mixed powder based 3Y-TZP are similar on the surface perpendicular and parallel to the magnetic field, as shown in Fig. 4(c) and (d), implying an isotropic microstructure even if the material showed crystallographic orientation.

3.3. Mechanical properties and toughening mechanism

The mechanical properties of the 3Y-TZP ceramics are summarized in Table 1. Whether textured or not, all sintered ceramics were fully dense with a comparable hardness of 1200–1300 kg/mm^2. With regard to toughness, there was a large difference between the co-precipitated and the mixed powder based 3Y-TZP. When formed in the absence of a magnetic field,

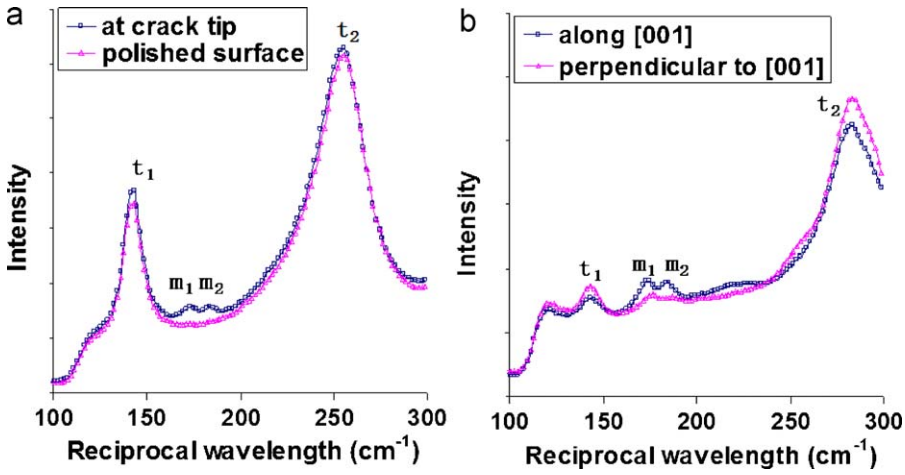

Fig. 6. Micro Raman spectra of the pristine polished surface and at the crack tip of a co-precipitated 3Y-TZP (a), and at the tip of crack perpendicular to and along the [0 0 1] direction of a textured 3Y-TZP (b) from the mixed SF-extra/TZ-8Y powder.

the toughness of the mixed powder based ceramic is 47.5% higher than that of the co-precipitated material. An enhanced toughness of 55% was also observed in 3Y-TZP prepared from yttria-coated m-ZrO_2.[27] From the correlation between the yttria distribution, t-ZrO_2 grain size distribution and the transformability of the ZrO_2 material, it could be concluded that the transformability and toughness of the yttria-coated ceramics was higher than that of the co-precipitated powder based yttria-stabilized zirconia because of the presence of a small amount of t-ZrO_2 grains with a low yttria content and a larger grain size.[27]

In the present work, a similar inhomogeneous yttria distribution in the starting powder mixture results in a sintered 3Y-TZP with a wider grain size distribution with a fraction of substantially larger grains compared to the co-precipitated equivalent, as shown in Fig. 4. The enhanced toughness obtained in the mixed powder based 3Y-TZP can therefore be attributed to the larger grains with lower yttria content. These larger grains are most probably originating from the larger fraction of m-ZrO_2 powder grains in the starting powder, which have a lower yttria content due to the longer time needed for interdiffusion of yttria from the originally smaller grained TZ-8Y starting powder.[3]

For the textured 3Y-TZP processed in the strong magnetic field, the toughness in the directions parallel and perpendicular to the magnetic field direction, was substantially different, as visually illustrated by the anisotropy in radial crack length originating at the corners of a Vickers indentation in Fig. 5(a). For comparison and reference, the symmetrical radial crack pattern of the co-precipitated 3Y-TZP is shown in Fig. 5(b). For the textured ceramic, the crack along the magnetic field direction is shorter than the crack perpendicular to the magnetic field direction. In other words, the toughness along the [0 0 1] direction is substantially higher. The numerical toughness values are summarized in Table 1. The textured powder mixed 3Y-TZP shows a toughness of 8.8 MPa $m^{1/2}$ along the magnetic field direction, and 5.7 MPa $m^{1/2}$ perpendicular to the magnetic field direction. This anisotropic toughness could not be attributed to the microstructure, which was isotropic, as shown in Fig. 4(c) and (d). Moreover, the lower toughness along the direction perpendicular to the [0 0 1] direction is comparable to the toughness of the non-textured mixed 3Y-TZP.

The tetragonal to monoclinic martensitic transformation is widely known to be the dominant toughening mechanism in 3Y-TZP ceramics. In order to assess the transformability of the t-ZrO_2 phase with regard to the direction and ceramic type, the phase constitution at the radial crack-tip of Vickers indentations on the polished co-precipitated and (0 0 1)-textured mixed powder based 3Y-TZP was studied by micro Raman spectroscopy, where the measured spots were indicated in Fig. 5.

The Raman spectrum of the pristine polished co-precipitated 3Y-TZP showed mainly two strong t-ZrO_2 peaks, as indicated by t_1 and t_2 in Fig. 6(a). In the spectrum measured at the crack tip of a Vickers indentation, two additional small m-ZrO_2 peaks[1] could be observed, as indicated by m_1 and m_2 in Fig. 6(a). This actually proves martensitic transformation activation at the crack-tip due to the stress applied during indentation. The spectra at the crack tips, along and perpendicular to the [0 0 1] direction, on the mixed powder based 3Y-TZP deposited in the presence of a magnetic field are compared in Fig. 6(b). Compared to the co-precipitated ceramic (Fig. 6(a)), the t_1 tetragonal peak decreased substantially whereas the m_1 and m_2 m-ZrO_2 peaks are significantly enhanced. Moreover, the m-ZrO_2 peaks in the Raman spectrum of the crack-tip along the [0 0 1] direction are more pronounced than perpendicular to the [0 0 1] direction of the textured ceramic, indicating that the t-ZrO_2 phase transformability on the textured 3Y-TZP along the [0 0 1] direction is enhanced. This is actually consistent with the higher toughness along the [0 0 1] direction in the textured 3Y-TZP discussed above (see Table 1). It is also noted that compared to the co-precipitated ceramic, the t_2 t-ZrO_2 peak of the mixed powder based 3Y-TZP shifts to the higher reciprocal wavelength numbers. Generally, the main factors that are responsible for the shift of Raman spectra are composition, crystal size and internal stress in the material.[29–31] As discussed above, the mixed powder based 3Y-TZP consists of the larger grains with lower yttria content and smaller grains with higher yttria content. The inhomogeneous yttria distribution in the mixed powder based 3Y-TZP with wider

particle size distribution may cause this Raman peak shift. Additionally, reactive sintering can create internal stresses in the synthesized 3Y-TZP, being another possible origin for this peak shift.

4. Conclusions

Monoclinic zirconia powder could be aligned in a magnetic field of 9.4 T with its (1 0 0) plane perpendicular to the magnetic field direction. The alignment of pure unstabilized m-ZrO_2 particles in a mixture of pure m-ZrO_2 and cubic 8Y-ZrO_2 in a magnetic field, deposited by EPD and densification by pressureless sintering allowed to obtain a textured 3Y-TZP ceramic. The microstructurally isotropic (0 0 1)-textured 3Y-TZP showed a substantial toughness anisotropy, with a toughness along the [0 0 1] direction 54% higher than perpendicular to the [0 0 1] direction. Moreover, the toughness along and perpendicular to the [0 0 1] direction is respectively 49% higher and comparable to that of the non-textured isotropic 3Y-TZP, prepared from the same powder. Raman spectroscopy allowed to correlate the enhanced fracture toughness to an enhanced t-ZrO_2 phase transformability that proved to be influenced by the crystallographic texture.

Acknowledgements

Financial support from the Flemish Institute for the Promotion of Scientific Technological Research in Industry (IWT) under contract SBO-PROMAG (60056) is gratefully acknowledged. The authors also acknowledge the support of the Research Fund of K. U. Leuven under project GOA/2008/007. We thank Mr. Murat Özen of the University of Antwerp for the helpful correspondence on the micro Raman measurements.

References

1. Chien FR, Ubic FJ, Prakash V, Heuer AH. Stress-induced martensitic transformation and ferroelastic deformation adjacent microhardness indents in tetragonal zirconia single crystals. *Acta Mater* 1998;**46**:2151–71.
2. Tsalouchou E, Cattell MJ, Knowles JC, Pittayachawan P, McDonald A. Fatigue and fracture properties of yttria partially stabilized zirconia crown systems. *Dent Mater* 2008;**24**:308–18.
3. Chevalier J, Gremillard L, Virkar AV, Clarke DR. The tetragonal–monoclinic transformation in zirconia: lessons learned and future trends. *J Am Ceram Soc* 2009;**92**:1901–20.
4. Gupta N, Mallik P, Basu B. Y-TZP ceramics with optimized toughness: new results. *J Alloys Compd* 2004;**379**:228–32.
5. Kelly PM, Francis Rose LR. The martensitic transformation in ceramics – its role in transformation toughening. *Prog Mater Sci* 2002;**47**:463–557.
6. Evans AG, Heuer AH. Transformation toughening in ceramics: martensitic transformations in crack-tip stress fields. *J Am Ceram Soc* 1980;**63**:241–8.
7. Venet M, Vendramini A, Santos IA, Eiras JA, Garcia D. Texturing and properties in hot forged SBN63/37 ceramics. *Mater Sci Eng B* 2005;**117**:254–60.
8. Xie R-J, Mitomo M, Kim W, Kim Y-W. Texture development in silicon nitride–silicon oxynitride in situ composites via superplastic deformation. *J Am Ceram Soc* 2000;**83**:3147–52.
9. Seabaugh MM, Kerscht IH, Messing GL. Texture development by templated grain growth in liquid-phase-sintered α-alumina. *J Am Ceram Soc* 1997;**80**:1181–8.
10. Suzuki TS, Sakka Y, Kitazawa K. Orientation amplification of alumina by colloidal filtration in a strong magnetic field and sintering. *Adv Eng Mater* 2001;**3**:490–2.
11. Sakka Y, Suzuki TS. Textured development of feeble magnetic ceramics by colloidal processing under high magnetic field. *J Ceram Soc Jpn* 2005;**113**:26–36.
12. Asai S. Magnetic crystalline alignment. *ISIJ Int* 2007;**47**:519–22.
13. Argyriou DN, Howard CJ. Re-investigation of yttria-tetragonal zirconia polycrystal (Y-TZP) by neutron powder diffraction – a cautionary tale. *J Appl Crystallogr* 1995;**28**:206–8.
14. Suárez G, Sakka Y, Suzuki T, Uchikoshi T, Aglietti EF. Texture development in 3 mol% yttria-stabilized tetragonal zirconia. *Mater Res Bull* 2009;**44**:1802–5.
15. Doungdaw S, Uchikoshi T, Noguchi Y, Eamchotchawalit C, Sakka Y. Electrophoretic deposition of lead zirconate titanate (PZT) powder from ethanol suspension prepared with phosphate ester. *Sci Technol Adv Mater* 2005;**6**:927–32.
16. Lotgering FK. Topotactical reactions with ferrimagnetic oxides having hexagonal crystal structures—I. *J Inorg Nucl Chem* 1959;**9**:113–23.
17. Matsumoto RLK. Evaluation of fracture toughness determination methods as applied to ceria-stabilized tetragonal zirconia polycrystal. *J Am Ceram Soc* 1987;**70**:366–8.
18. Anstis GR, Chantikul P, Lawn BR, Marshall DB. A critical evaluation of indentation techniques for measuring fracture toughness: I. Direct crack measurements. *J Am Ceram Soc* 1981;**64**:533–8.
19. Hannink RHJ, Kelly PM, Muddle BC. Transformation toughening in zirconia-containing ceramics. *J Am Ceram Soc* 2000;**83**:461–87.
20. Hayakawa M, Kuntani N, Oka M. Structural study on the tetragonal to monoclinic transformation in arc-melted ZrO_2–2 mol% Y_2O_3—I. Experimental observations. *Acta Metall* 1989;**37**:2223–8.
21. Hayakawa M, Oka M. Structural study on the tetragonal to monoclinic transformation in arc-melted ZrO_2–2 mol% Y_2O_3—II. Quantitative analysis. *Acta Metall* 1989;**37**:2229–35.
22. Hayakawa M, Adachi K, Oka M. Crystallographic analysis of the monoclinic herringbone structure in an arc-melted ZrO_2–2 mol% Y_2O_3 alloy. *Acta Metal Met Mater* 1990;**38**:1753–9.
23. Zhang L, Vleugels J, Van der Biest O. Slip casting of alumina suspensions in a strong magnetic field. *J Am Ceram Soc* 2010;**93**:3148–52.
24. Kimura T, Takahashi T, Tani T, Saito Y. Crystallographic texture development in bismuth sodium titanate prepared by reactive-templated grain growth method. *J Am Ceram Soc* 2004;**87**:1424–9.
25. Takeuchi T, Tani T, Saito Y. Unidirectionally textured $CaBi_4Ti_4O_{15}$ ceramics by the reactive templated grain growth with an extrusion. *Jpn J Appl Phys* 2000;**39**:5577–80.
26. Tajima S, Tani T, Isobe S, Koumoto K. Thermoelectric properties of highly textured $NaCo_2O_4$ ceramics processed by the reactive templated grain growth (RTGG) method. *Mater Sci Eng B* 2001;**86**:20–5.
27. Vleugels J, Yuan ZX, Van der Biest O. Mechanical properties of Y_2O_3/Al_2O_3-coated Y-TZP ceramics. *J Eur Ceram Soc* 2002;**22**:873–81.
28. Lange FF. Transformation-toughened ZrO_2: correlations between grain size control and composition in the system ZrO_2–Y_2O_3. *J Am Ceram Soc* 1986;**69**:240–2.
29. Cheng YH, Tay BK, Lau SP, Kupfer H, Richter F. Substrate bias dependence of Raman spectra for tin films deposited by filtered cathodic vacuum arc. *J Appl Phys* 2002;**92**:1845–9.
30. Sobol AA, Voronko YK. Stress-induced cubic-tetragonal transformation in partially stabilized ZrO_2: Raman spectroscopy study. *J Phys Chem Solids* 2004;**65**:1103–12.
31. Teixeira V, Andritschky M, Fischer W, Buchkremer HP, Stöver D. Analysis of residual stresses in thermal barrier coatings. *J Mater Process Technol* 1999;**92–93**:209–16.